ISSN 1330-3651 (Print), ISSN 1848-6339 (Online)
https://doi.org/10.17559/TV-20240219001335
Original scientific paper

Optimal Integration of Wave Energy Converters in the Vis Island Renewable Microgrid

Blaž JOZANOVIĆ, Irina TEMIZ, Damir ŠLJIVAC, Branka NAKOMČIĆ-SMARAGDAKIS*

Abstract: In order to demonstrate the viability of wave energy converters usage in the Mediterranean islands, this paper explores the possibilities of optimized technical integration of wave energy converters into an island's electrical grid, with a particular focus on the island of Vis in the Adriatic Sea. After introduction, a comprehensive definition of wave energy was provided and classifications and technologies associated with wave energy converters were discussed. Additionally, different interface types between wave energy converters and the grid were discussed, as well as the potential impact of these converters on the island's grid and its electrical power system. Power matrices of two different wave energy converters (WECs), namely Wavestar and Wavebob, were adjusted to the specific sea conditions around Vis using the Froude scaling method. Also, Power Factory software tool was used to model the island's power grid, conduct simulations, and present electrical parameter values derived from real-world data collected on Vis. Various scenarios involving the integration of photovoltaic power plants and wave energy converters with the resulting data are both visually and numerically presented. Simulation results indicate a successful possibility of integrating wave energy converters to the microgrid of the island of Vis with the aim to archive near net zero electricity exchange with the mainland grid with improved power (voltage) quality in the island microgrid.

Keywords: distribution grid; Mediterranean islands; optimal integration; renewable island microgrid; wave energy; wave energy converters

1 INTRODUCTION

The reliance on traditional energy sources, such as fossil fuels and imported natural gas, has exposed European countries to potential supply disruptions and price volatility. There is a growing recognition of the importance of diversifying energy sources and strengthening energy security by introducing renewable energy sources (RES), such as wind, geothermal, solar, wave and other ocean energy.

Wave energy refers to the capture and conversion of the energy present in sea and oceanic waves into a usable form of power. It refers to the kinetic energy generated by waves as they propagate across the water surface. Devices that convert wave energy into usable forms of power are called wave energy converters (WECs). Wave energy has been regarded as a highly promising renewable energy source for a considerable period of time. It stands out not only for its abundant energy potential but also for its superior reliability compared to many other renewable energy sources. Wave power can be harnessed at a specific location up to 90 percent of the time, whereas solar and wind energy tend to be available for only 20 - 30 percent of the time [1]. The field of wave energy has seen big advancements in the last decades and there are a lot of concepts for various wave energy devices, with several of them showcasing the potential for economically feasible electricity generation. Wave energy potential exists throughout every shore so it is particularly interesting for isolated communities, such as islands.

Vis Island, located in the waters of the Adriatic Sea, is the farthest meaningfully inhabited island on the Croatian coastline. It is connected to the mainline grid and is a big summer tourist attraction with high energy summer consumption. Authors already presented technical possibilities and cross-cutting aspects of the integration of wave power farms into power systems of the Adriatic islands in [2]. This paper focuses now on the optimal operation of wave energy conversion systems in the RES microgrid of Mediterranean islands. The island RES microgrid, consisting of local energy generation, storage, and distribution systems, offers an opportunity to integrate wave energy into the existing energy infrastructure of the island, enhancing its energy stability and fostering greater energy autonomy.

The primary objective is to develop an optimized operational strategy for wave energy conversion systems in the hybrid microgrid, taking into account various factors such as wave conditions, energy demand patterns, already existing energy distributed generation, and system limitations. Hybrid-microgrid planning, sizing and optimization has been described in [22].

By maximizing the utilization of wave energy resources and ensuring efficient energy management, the proposed operational strategy should aim to enhance the overall performance, stability, and reliability of the microgrid while archiving close to net zero exchange of energy with the mainland grid. Through a multidisciplinary approach, the research seeks to contribute to the advancement of renewable energy practices and provide practical solutions for the sustainable development of island communities.

Specific goals in the case study described in the paper are to define the wave power potential for chosen sites near the island of Vis and model them using the JONSWAP Adriatic wave spectrum, model Wave power farms and photovoltaic farm (RES microgrid) and their integration to the local distribution grid in order to assess their technical viability.

2 DEFINING WAVE ENERGY AND WAVE ENERGY CONVERTERS

2.1 Wave Energy Definition

Sea waves at any location consist of various wave fields, including wind-generated waves and swells. The average energy density per unit horizontal surface area is calculated using the Eq. (1):

$$E = \frac{1}{16}\rho g H_s^2 \tag{1}$$

For deep water, the group velocity, which represents the speed of energy transport, is equal to:

$$c_g = \frac{1}{4\pi} g T_e \tag{2}$$

Therefore, the wave power per unit of wave front length is obtained as the product of average energy density and group velocity and is defined as:

$$P = \frac{1}{64\pi} \rho g^2 H_s^2 T_e \tag{3}$$

where ρ is the saltwater density, g is the gravitational acceleration, H_s is the significant wave height, and T_e is the wave energy period. From Eq. (2) and Eq. (3), it is evident that the propagating wave height and period determine the available wave power at a given location, and therefore, wave characteristics are significantly influenced by changes in bathymetry from open sea to coastal areas [3]. Through furred formulation given by researchers of [4] the significant wave height and energy period can be obtained from the wave power spectrum $S(\omega)$ via spectral moments m_n:

$$m_n = \int_0^\infty S(\omega)\omega^n \mathrm{d}\omega \tag{4}$$

where ω is the angular wave frequency and the significant wave height and the wave energy period are:

$$H_s = 4\sqrt{m_0} \tag{5}$$

$$T_e = \frac{m_{-1}}{m_0} \tag{6}$$

Further, along the Croatian coastline, the wave power potential was assessed by [5]. The JONSWAP wave spectrum was optimized for the Adriatic Sea as:

$$s(\omega) = 0.8626 \frac{5}{16} \frac{H_s^2 \omega_m^4}{\omega^5} \exp\left[-\frac{5}{4}\left(\frac{\omega_m}{\omega}\right)^4\right] 1.78^{\exp\left[-\frac{1}{2}\left(\frac{\omega-\omega_m}{\sigma\omega}\right)^2\right]} \tag{7}$$

where: $\omega_m = 0.52 + \frac{1.4}{H_s + 0.7}$ is the modal frequency and $\sigma \begin{cases} \sigma_a = 0.06 \text{ for } \omega \le \omega_m \\ \sigma_b = 0.08 \text{ for } \omega > \omega_m \end{cases}$ is the measure of spectral width from the spectral peak.

Alternatively, T_e can be estimated based on the peak wave period T_p using the JONSWAP wave spectrum for the Adriatic Sea as:

$$T_e = \alpha T_p \tag{8}$$

where coefficient α depends on the shape of the wave spectrum. In this case, it corresponds to $\alpha = 0.8626$.

2.2 Wave Energy Converters

Wave energy converters (WECs) differ not only by shape and size but also by the type of materials used in their construction, their environmental impact, conversion chain efficiency, and many other characteristics. WECs can be categorized based on their wave capture method or operational mode. They can also be classified according to water depth and distance from the shore. Based on the distance from shore, WECs can be divided into onshore devices, nearshore devices, and offshore devices [1, 6]. Based on wave incident direction, WECs can be classified as attenuators, point absorbers, and terminators. Furthermore, based on the working principle, WECs can be divided into oscillating wave column (OWC) WECs, overtopping WECs, and oscillating bodies.

2.2.1 Types of Connections of WEC to the Power Grid

Distributed generators, in general, can be connected to the grid in multiple ways. There is direct coupling with the grid, indirect coupling which is done with power electronic coupling (it can be fully or partially coupled over power electronics), and also modular (distributed) power electronic interface, which, in this context, connects to a number of generators that are connected to the same local grid through power electronics converters. If such units belong to the same owner, their operation can be coordinated in a way to achieve certain benefits, for example, regulating the local voltage level.

Fig. 1 underscores the multitude of techniques available for harnessing wave energy and that variations in generator designs are evident, encompassing a variety of turbine types such as Wells, impulse, and propeller turbines. The choice of turbine type is contingent upon factors like wave power and the necessary rotation speed for optimal generator operation. Moreover, the inclusion of accumulators and water reservoirs is also a plausible consideration.

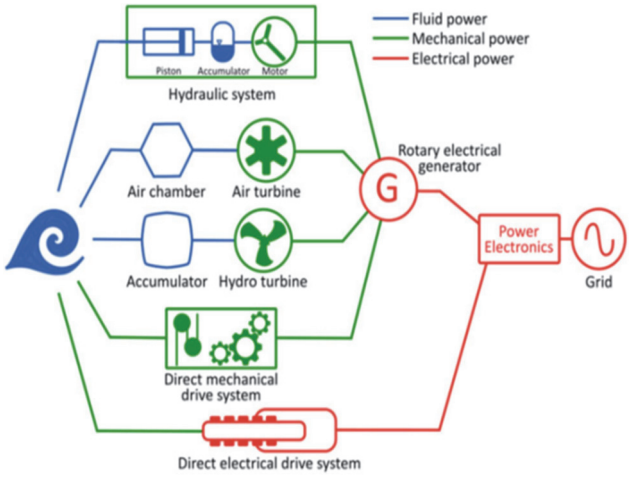

Figure 1 Types of WEC connections to the grid [12]

An essential aspect to note is that for connecting WEC systems to the power grid, power electronics or power transformers are used in most cases. Their role is the efficiency optimisation of transferred power to the grid and to control the above-mentioned transfer of power to satisfy the power grid conditions.

In general, WEC type of connection has an impact on:
- Power flow, where the grid becomes active rather than passive.
- Power quality: the electrical conditions within a network encompass power flows, current loads, losses, voltage scenarios, regulation, short-circuit currents, and system reliability and stability. The quality of the electric energy generated from a power plant (distributed source) involves the requirement of a certain quality standard by the distribution or transmission system operator, as defined by the HRN EN 50160 norm in Croatia and the EU including voltage variations, transients, harmonic distortion, flickers, and more [13, 14].
- Efficiency of electricity production, influenced by connection technology and manufacturer choice but also by nominal power and technology management such as modular electronic power converters in systems, results in higher efficiency compared to singular high-power converters.
- Costs of electric energy production (LCOE), are impacted by production efficiency and investment, maintenance, and operational costs throughout the systems lifecycle, where technology robustness plays a significant role.
- Complexity and control (regulation) capabilities of WECs: additionally, the complexity and control potential (regulation) of a power plant (distributed generator, DG) are crucial as having a complete connection with electronic power converters of nominal power enables optimal and independent management of active and reactive power injected into the grid [13, 14].

2.3 Impact of WEC Distributed Generation on the Grid

The integration of DG can potentially introduce disruptions within the power system, necessitating additional financial investments to address these issues. The given impact depends on the starting grid conditions and grid hosting capacity, where the hosting capacity of the distribution grid refers to its ability to accommodate or absorb a certain amount of energy from the DG without exceeding the operational limits or constraints of the system. It can be defined as the maximum amount of energy that the distribution network can safely integrate from the DG at the point of common coupling without causing any violations or disruptions to the system's operation. Possible impacts of WEC distributed generation on the electrical power system are changes in power flow, voltage magnitude variations, overloading and losses and power quality disturbances [14].

2.3.1 Changes in Power Flow

Integrating WECs into the power grid results in changes to power flow, meaning that the grid becomes active rather than passive. It can be seen that power flow is determined by the localised difference between current demand and current supply of energy. Based on this understanding one can conclude that the maximum energy production from WECs should be kept below the sum of the minimum consumption and the highest permissible power flow through the distribution network. This ensures that there is no overload in the upstream grid.

2.3.2 Voltage Variations and Power Quality

The potential effects of integrating wave power farms must be carefully considered. As a result, there are restrictions on the maximum number of distributed sources, notably WECs, and the maximum power capacity that can be incorporated into the facility. Restrictions are imposed on the integration of renewable energy sources due to changes in voltage levels between grid components, particularly instances of considerable voltage rise. The likelihood of voltage rise is dependent on variables like the distributed generator or source's power output and location. Upon connecting a distributed generator to the grid there is an accompanying elevation in voltage at the generator's terminals. The proportional increase in voltage can be estimated using the following expression:

$$\Delta u_{gen} = \begin{cases} L \cdot \dfrac{R \cdot P_{gen}}{u_{nom}^2}, L \le L_{gen} \\ L_{gen} \cdot \dfrac{R \cdot P_{gen}}{u_{nom}^2}, L \ge L_{gen} \end{cases} \tag{9}$$

where R represents the source resistance at the generator's terminals, P_{gen} denotes the injected active power, and U_{nom} signifies the nominal voltage. This approximation is applicable in practical scenarios at the distribution level.

Voltage variation, particularly increases in voltage, pose a more significant constraint on the potential level of integration than power flows. Interestingly, the most challenging situations arise during periods of minimal load rather than peak demand. In order to increase the level of integration, voltage variations can be influenced by the following methods [14]:
- Tap Changers with Line-Drop Compensation.
- Building new power lines/transformers or increasing cross-section of power line/power of transformers.
- Regulating the active and reactive power output of WECs.
- Combination of methods.

Allowed limits for the given voltage increases or decreases are given by European norm EN 50160 which defines and describes the essential characteristics of the supply voltage at the point of delivery to consumers in public low-voltage, medium-voltage and high-voltage networks under normal operating conditions. In this norm it is also defined what should be taken into account in regard to voltage quality when implementing WECs into the distribution network. Integration of WECs has a benefit in regard to particular disturbances as voltage fluctuation, voltage dips and harmonics. A voltage source in the distribution system makes the grid more resilient and negates the disturbances.

By actively managing the reactive power flow between the generator and the grid, it is possible to regulate the voltage at the generator unit's terminals. This is feasible when synchronous machines or generators with power electronics interfaces are utilized. While managing the active power flow, voltage dips and fluctuations can be dampened, and by utilising advanced controls on modern power electronic converters, harmonic distortion can be mitigated either by simply compensating the downstream

harmonic emissions by employing open-load control or also by actively using the resonance frequency of the harmonics to dampen them [14].

2.3.3 Overloading and Losses

While designing a power grid, especially power lines and protection elements, thermal endurance of components is a vital aspect to consider. It does not only depend on power flows through components, and consequently electrical currents, but it also depends on environmental conditions i.e., air temperature, snow, rain, wind, solar irradiation, etc. Hence, a special consideration is required when integrating WEC into the power grid because certain changes are happening in the grid such as changes in current value and changes in short-circuit current value [14].

Power lines and cables are usually oversized in terms of thermic limits; however, to limit overloading and losses on certain elements of the grid and to enhance the integration capacity of WECs, there are methods to mitigate these issues: enhancing the capability of loading power lines/cables, dynamic capability of loading and building new power lines/cables, dynamic longitudinal and transverse compensation, energy management systems, demand and energy storage systems and reconfiguration and enhanced protection [14].

3 METHODOLOGY AND MODELS

This section provides an explanation of the tools and assumptions employed to reach the goals of this paper. Locations and sea states will be discussed and evaluated. A detailed explanation is provided for the devices and the adaptation of ratings for the power matrices and lastly, the modelled grid and case studies will be examined.

3.1 Wave Climate and Wave Energy Potential Around the Island of Vis

The wave climate of the Adriatic Sea is predominantly influenced by its geographical location and surrounding topography. The majority of the Adriatic Sea is characterized by a Mediterranean climate type. It is divided into three regions looking from north to south: the upper Adriatic Sea, the middle, and the lower Adriatic Sea, subdivided into 28 grid cells (Fig. 2), each representing 1 degree of longitude and 1 degree of latitude. The island of Vis is situated in the central Adriatic Sea, located at the intersection of grid cells 11, 12, 16, and 17.

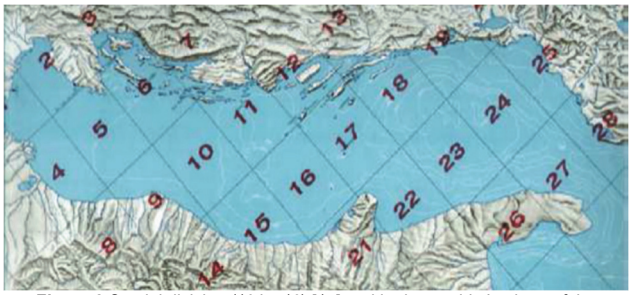

Figure 2 Spatial division (1° by 1°) [15] and hydrographic Institute of the Republic of Croatia

Utilizing data from the Copernicus Climate Data Store program, specifically ERA5 hourly data on single levels for the year 2012 [16], a matrix of size 7 × 5 × 8784 was obtained. In this matrix, the first number represents longitude, the second represents latitude, and the third corresponds to the number of hours in the observed year.

During data analysis, the initial step involved excluding locations that were too far from the island and removing locations with missing data (NaN values). Subsequently, two nearby locations near the island of Vis remained for further analysis (Fig. 3 and Tab. 1).

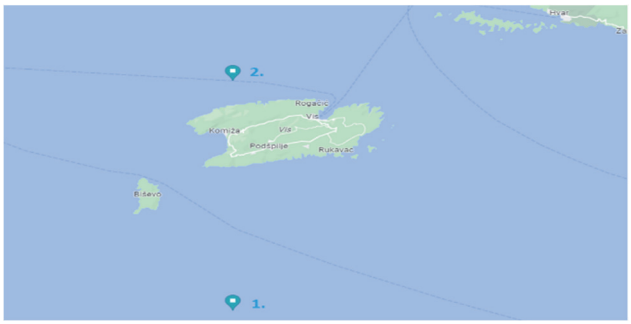

Figure 3 Map representation of chosen locations 1 and 2 source: https://www.google.hr

Table 1 Geographical coordinates for the chosen locations in the Adriatic Sea with the corresponding depth of the water and the distance from shore. Bathymetry data [17]

Location	Latitude	Longitude	Water Depth / m	Distance from shore / km
1.	42.85	16.10	128	17.60
2.	43.10	16.10	102	3.5

In total, two such matrices were acquired, one encompassing detail related to significant wave height calculated from spectral moments and the other containing information about peak wave periods. Tables have been created to organize the occurrences of significant wave height and energy wave period into classes for a specific location. The significant wave height classes are categorized in meters, with an increment of 0.5 m per class ranging from 0 to 5.5 m. Similarly, energy period classes are defined with 1-second increments ranging from 0 to 9 seconds. Based on a dataset consisting of 8784 data logs, the number of different sea states are presented in Tab. 2 and Tab. 3, representing the sea states of location 1 and location 2, respectively.

It can be observed that selected locations around Vis Island are characterized by predominantly calm sea states. Consequently, this indicates the necessity for downsizing WECs to suit these milder wave conditions. The data from Tab. 3, Tab. 4 and Tab. 5 suggest that the WECs need to be optimized and adapted to efficiently harness energy from the relatively tranquil sea states observed in the chosen locations. Due to the geographical positioning, location 1situated to the south of the island more distanced from coastline and location 2 positioned to the north of the island in closer proximity to the shore, displaying distinct variations in wave conditions.

Table 2 Wave climate scatterplot for location 1

H_s/T_e	0 - 1	1 - 2	2 - 3	3 - 4	4 - 5	5 - 6	6 - 7	7 - 8	8 - 9	9 - 10	10 - 11	Σ
0 - 0.5	0	383	2188	901	197	10	19	13	0	0	0	3711
0.5 - 1	0	0	252	1907	793	168	11	11	9	5	0	3156
1 - 1.5	0	0	0	176	667	163	41	17	0	2	5	1071
1.5 - 2	0	0	0	1	190	251	53	12	0	0	0	507
2 - 2.5	0	0	0	0	14	136	32	37	0	0	0	219
2.5 - 3	0	0	0	0	0	31	24	15	0	0	0	70
3 - 3.5	0	0	0	0	0	0	23	5	0	0	0	28
3.5 - 4	0	0	0	0	0	0	6	5	0	0	0	11
4 - 4.5	0	0	0	0	0	0	1	6	0	0	0	7
4.5 - 5	0	0	0	0	0	0	0	4	0	0	0	4
5 - 5.5	0	0	0	0	0	0	0	0	0	0	0	0
Σ	0	383	2440	2985	1861	759	210	125	9	7	5	8784

Table 3 Wave climate scatterplot for location 2

H_s/T_e	0 - 1	1 - 2	2 - 3		3 - 4	4 - 5	5 - 6	6 - 7	7 - 8	8 - 9	9 - 10	10 - 11	Σ
0 - 0.5	0	544	2817		1090	388	64	14	5	2	1	0	4925
0.5 - 1	0	0	414		1277	606	263	16	13	6	7	5	2607
1 - 1.5	0	0	0		151	436	185	27	17	0	0	0	816
1.5 - 2	0	0	0		4	114	130	27	21	0	0	0	296
2 - 2.5	0	0	0		0	10	55	14	15	0	0	0	94
2.5 - 3	0	0	0		0	0	10	16	4	0	0	0	30
3 - 3.5	0	0	0		0	0	0	8	5	0	0	0	13
3.5 - 4	0	0	0		0	0	0	0	3	0	0	0	3
4 - 4.5	0	0	0		0	0	0	0	0	0	0	0	0
4.5 - 5	0	0	0		0	0	0	0	0	0	0	0	0
5 - 5.5	0	0	0		0	0	0	0	0	0	0	0	0
Σ	0	544	3231		2522	1554	707	122	83	8	8	5	8784

Table 4 Wave climate of the chosen locations [16]

Location	$H_{S,\max}$ / m	$H_{S,\text{mean}}$ / m	$T_{e,\max}$ / s	$T_{e,\text{mean}}$ / s	E_{wave} / MWh
1	4.8529	0.7250	10.2529	3.6585	75177.3083
2	3.5613	0.5761	10.3142	3.4121	45017.87635

3.2 Modelling oh Wavestar and Wavebob WECs

A pair of distinct WECs has been chosen for analysis, considering their performance characteristics and the depth of their mooring installations, which goes to a 100 m. These converters were subject to the Froude scaling technique in order to harmonize their behaviour with the distinct sea states of the Adriatic Sea [18]. This involved primarily focusing on the reduction of the wave height parameter to align with the requisite sea state criteria and consequently reducing the time and power parameters with their respective scaling conversion factors as in Tab. 5. Due to downscaling, removal of excess rows and columns was necessary because some rows will have two or more values. The surplus values were removed, leaving just one value.

Table 5 Froude scaling conversion factors

Parameter	Scaling factor
Angle	λ^0
Angular acceleration	λ^{-1}
Force	λ^3
Linear acceleration	λ^0
Mass	λ^3
Moment	λ^4
Length	Λ
Power	$\lambda^{7/2}$
Pressure	Λ
Time	$\lambda^{1/2}$
Velocity	$\lambda^{1/2}$

The interpolation technique is used to carry out this process. The first power matrices were designed for 15000 kW for Wavestar converter and 1000 kW for Wavebob converter, and as a result, the succeeding matrices obtained by using the Froude law may be influenced by this initial optimization, leading to potential changes. While scaling the converters, the depth of mooring should ideally be proportionally adjusted. For the purpose of this study, the mooring depth remains unaltered from its pre-scaling value. Also, given the specific focus of this paper, which revolves around the influence of wave power on the power system, particularly the distribution grid of the islands, it is imperative to note that the present analysis does not encompass hydrodynamic interactions between WECs.

Wavestar employs a Hydraulic Motor Power Take-Off system. This device is composed of multiple floats linked to a singular structure positioned on the seabed. This solitary structure serves as a stable reference point for the Wavestar system (Fig. 4).

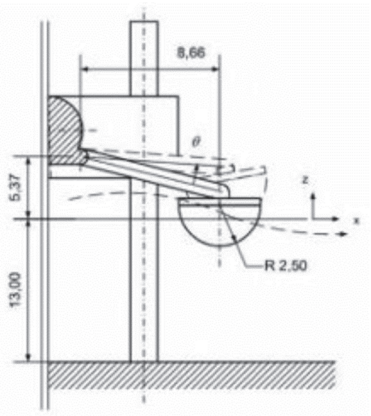

Figure 4 Wavestar schematics [19]

Wavebob is classified as an axisymmetric WEC integrated with a Hydraulic Motor Power Take-Off system. Moreover, Wavebob employs a mooring system securely

anchored to the seabed, contributing to the overall structural stability (Fig. 5).

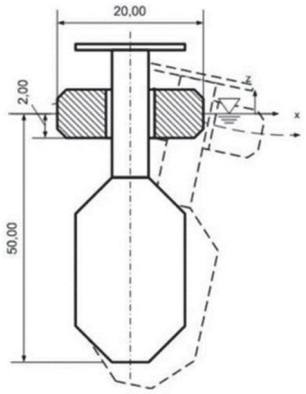

Figure 5 Wavebob schematics [19]

The C8-15000 kWWavestar concept served as the initial reference point, it consisted of 60 floats of 8 m diameter each, along with its corresponding power matrix as illustrated in Tab. 6 in which the output power is rated in kW, Hs is the significant wave height measured in meters and Te is the wave energy period measured in seconds. The Froude scaling method was employed, utilizing a scaling factor of 0.26827. Subsequent to scaling, the resultant output power of the aforementioned converter was computed hourly for the stipulated year, encompassing both case locations. The outcome of this computation is graphically represented in Fig. 6.

The associated power matrix of Wavebob converter is presented in Tab. 7 outlining the output power measured in kW, with H_s representing the significant wave height in meters, and T_p denoting the peak wave period in seconds. As it was done with Wavestar, the same application of the Froude scaling technique was used, utilizing a scaling factor of 0.25, the output power of the Wavebob converter for the designated year is visually portrayed in Fig. 7.

3.3 Modelling the Vis Island Microgrid

The model of the VIS island power grid was simulated using authentic data, for the year 2012, and schematics obtained from Hrvatska Elektroprivreda, the Croatian Operator of the Distribution System (HEP ODS) [20], the microgrid using DIgSILENT's advanced power system analysis software application PowerFactory.

The Vis island microgrid is powered by two cable ducts, specifically "KK Točila 35 kV" and "KK Stenjalo 35 kV," which establish a connection between the substations "TS Stari Grad 110/35 kV" and "TS Hvar 35/10 kV" located on the neighbouring island of Hvar, and the substation "TS Vis 35/10 kV" on the Vis island. The mentioned substation on Vis Island serves as a central distribution point for the supplied energy. Within the microgrid, energy is distributed through a network of interconnected powerlines, totalling three main routes and their subsidiaries. These powerlines then connect to 54 transformer substations that connect the medium voltage grid to the low voltage grid.

In addition to the substations, the network includes a photovoltaic (PV) power plant, rated nominal power of 3,5 MW [20] connected to the grid over 5 inverters of 720 kWp each and with a 1 MW battery. In the PV power plant, there are 11.200 PV modules of 340 Wp. Static generator is used for modelling the WEC and also an adjacent battery storage system. In this paper, the impact of integrating WECs on the grid will be observed in the course of a leap year.

As depicted in Fig. 8, it becomes evident that the island's energy consumption exhibits significant variability, fluctuating in accordance with the changing seasons with the highest consumption rates occurring during the summer months, which coincide with the tourist season. The spikes throughout the year are unknown anomalies and it is unknown if they are caused due to issues upstream in the grid or are just measuring errors.

Table 6 Wavestar performance matrix [19]

H_s/T_e	0 - 1	1 - 2	2 - 3	3 - 4	4 - 5	5 - 6	6 - 7	7 - 8	8 - 9
0 - 0.5	0	0	0	51	141	238	308	308	352
0.5 - 1	0	0	124	336	658	982	1165	1242	1243
1 -1,5	0	0	275	748	1459	2144	2490	2597	2549
1.5 - 2	0	89	551	1495	2899	4012	4386	4388	4196
2 - 2.5	0	145	895	2424	4665	6118	6461	6308	5935
2.5 - 3	0	212	1308	3535	6757	8462	8713	8358	7766
3 - 3.5	0	299	1846	4916	9230	11103	11189	10575	9729
3.5 - 4	0	395	2438	6425	11895	13860	13742	12850	11743
4 - 4.5	0	507	3126	8160	14913	15000	15000	15000	13838
4.5 - 5	0	634	3912	10072	15000	15000	15000	15000	15000

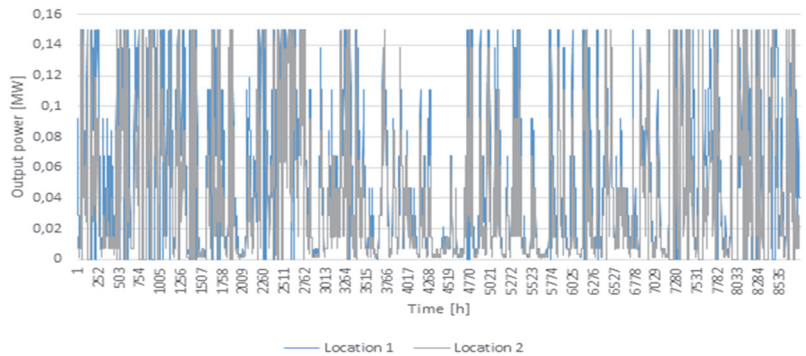

Figure 6 Wavestar yearlong output power for both case locations

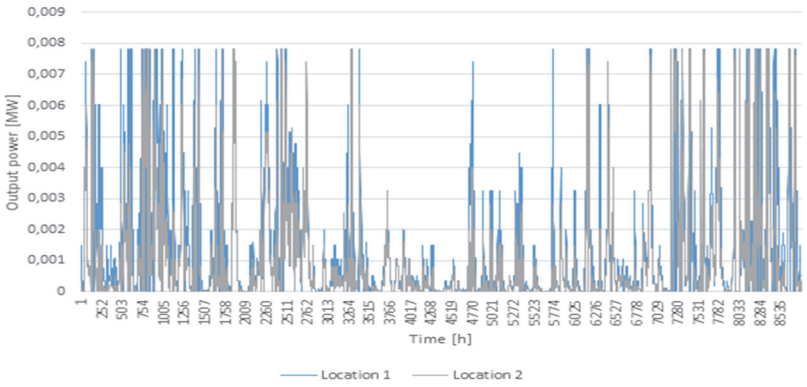

Figure 7 Wavebob yearlong output power for both case locations

Table 7 Wavebob performance matrix [19]

H_s/T_p	4	5	6	7	8	9	10	11	12
1	6	11	19	25	30	44	50	53	44
1.5	13	25	43	55	68	90	102	92	91
2	24	45	65	100	121	153	175	151	122
2.5	0	65	104	141	191	179	243	255	190
3	0	96	137	205	244	357	293	353	260
3.5	0	0	192	254	291	431	385	424	314
4	0	0	256	366	403	551	536	531	473
4.5	0	0	327	418	574	678	708	665	509
5	0	0	358	514	658	824	828	618	638
5.5	0	0	0	610	774	880	936	905	805
6	0	0	0	771	952	974	1000	838	886
6.5	0	0	0	788	1000	1000	1000	979	1000
7	0	0	0	781	1000	1000	1000	1000	1000

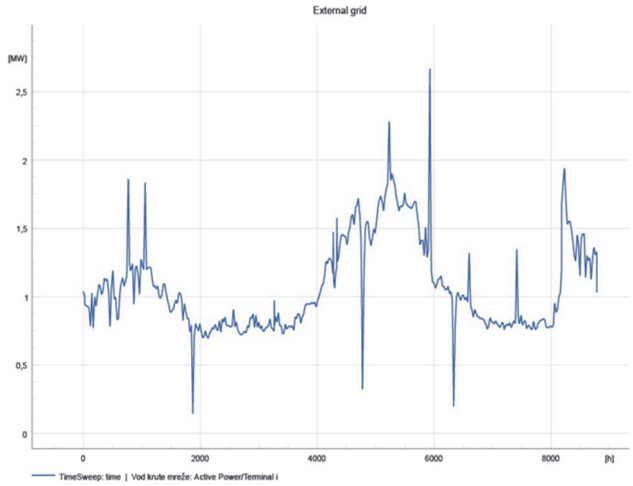

Figure 8 "35/10 kV Vis" transformer substation load curve, source HEP

The positioning of the WEC has been strategically arranged to replicate their real-world deployment (Fig. 9). In the context of location 1, the WECs are linked through a 1,5 MVA 0,4/10 kV transformer, establishing a connection to the terminal (TRM) labelled "Podšpilje-Dračevo polje" via a 10 kV N2XSEY XLPE PVC 3 × 50 mm underwater cable. Correspondingly, the WECs situated at location 2 follow a similar pattern, being connected to a terminal named "Oključna 2".

In the PowerFactory, a time sweep analysis was conducted to obtain voltage, true power, reactive power, and apparent power curves with respect to the time of year. This simulation was carried out in one-hour intervals, aligning with the one-hour steps of ERA 5 data. As a result, both PV and WEC distributed generation curves are presented in resolutions of one hour. The PV curves are indicated in kW, while the WEC curves are expressed in MW. Similarly, transformer substation load curves were provided in MVA and also maintained a one-hour resolution.

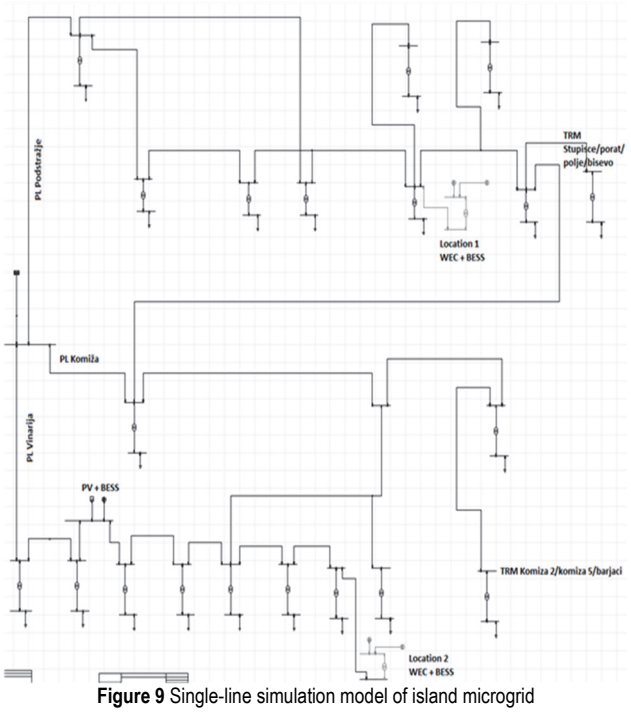

Figure 9 Single-line simulation model of island microgrid

As for the photovoltaic (PV) power plant modelled, its output power was calculated as in [21] by:

$$P_{array,t} = P_{mod,STC} \cdot \frac{G_t}{G_{STC}} \cdot \frac{\eta_{inv}}{100} \cdot \left(1 - \frac{\gamma}{100} \cdot \left(t_{mod,t} - t_{STC}\right)\right) \cdot N_{mod} \quad (10)$$

where $P_{array,t}$ stands for the AC power output of a PV array in kW, while $P_{mod,STC}$ refers to the peak power of one module; G_t represents the measured solar irradiance value W/m^2, with G_{STC} W/m^2 set at a value of 1000; η_{inv} signifies the inverter efficiency, which in this case is 97,5%; γ denotes the power temperature coefficient, equating to 0.38 %/°C in this context and N_{mod} refers to the number of modules in a string; t_{STC} is 25 °C and $t_{mod,t}$ signifies the calculated temperature in °C by:

$$t_{mod,t} = t_{amb} + \frac{NOCT - 20}{800} G_t \tag{11}$$

where t_{amb} / °C is the ambient temperature and $NOCT$ stands for Normal Operating Cell Temperature, set at 44 °C.

4 RESULTS OF ISLAND MICROGRID SIMULATION CASES

Power flows and voltage profiles were monitored along the designated terminal buses and feeders (power lines) to determine distributed generation (DG) influence both at the point of common coupling (PCC) and deeper in the grid. Performed case studies investigate the following scenarios:

- Island microgrid prior to (any) integration of distributed generation.
- Island microgrid with an integrated photovoltaic (PV) power plant and battery storage system (BESS). i.e. current situation.
- Island microgrid with an integrated photovoltaic power plant and battery storage system, along with a WEC power plant for two different locations and two types of WECs.
- Island microgrid with an integrated photovoltaic power plant and battery storage system, along with a WEC power plant for two different locations and two types of WECs, along with an adjacent BESS within the WEC power plant.

4.1 Island Microgrid Simulation Prior to Integration of Distributed Generation

Prior to integration of distributed generation (passive grid) it is evident that the grid exhibits an inductive nature, resulting in voltage progressively decreasing (Fig. 10). All the load supplied from the neighbouring island of Hvar amounts to 9415 MWh. The load curve exhibits peak spikes, with the highest recorded load reaching 2.73 MW.

Figure 10 Island microgrid terminal buses voltage levels prior to DG integration

Fig. 11 displays the distribution of active loads along the main feeders, revealing that the highest load is concentrated on the feeder "Komiža," whereas the lowest load is observed on feeder "Podstražje" with clear correlation between power line loads and consumption down the lines. The red curve in Fig. 11 portrays the reactive power output from island to the upstream network.

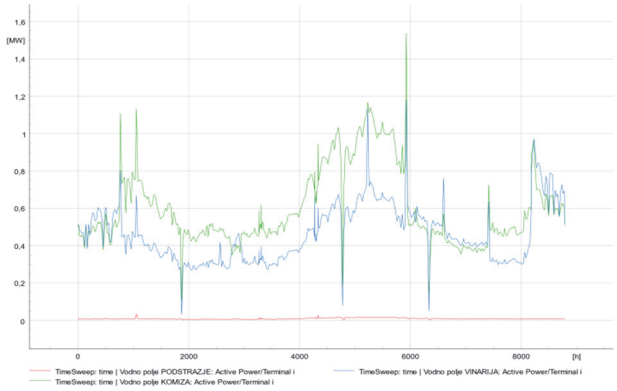

Figure 11 Island microgrid feeders power flows prior to DG integration

4.2 Island Microgrid Simulation with anl PV Power Plant and Battery Storage System (Current Situation)

In this particular scenario the battery storage system was simulated using a "static generator" block with a time-based characteristic in PowerFactory. By integration of PV power plant magnitudes of voltage, power flows are rising (Fig. 12 and Fig. 13). Voltage levels at terminal buses have slightly wider range then before the integration but within permissible power quality range specified by EN 50160 norm.

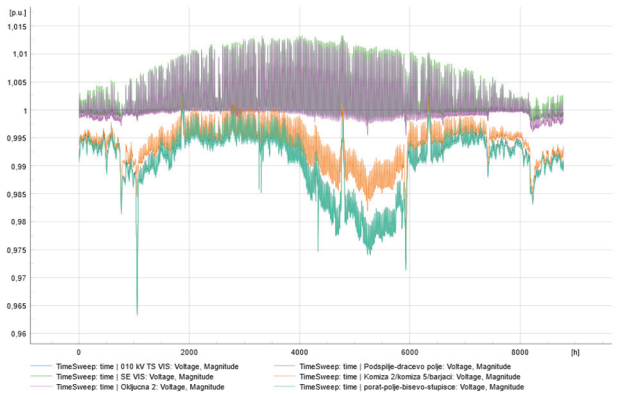

Figure12 Island microgrid terminal buses voltage levels after PV+BESS integration

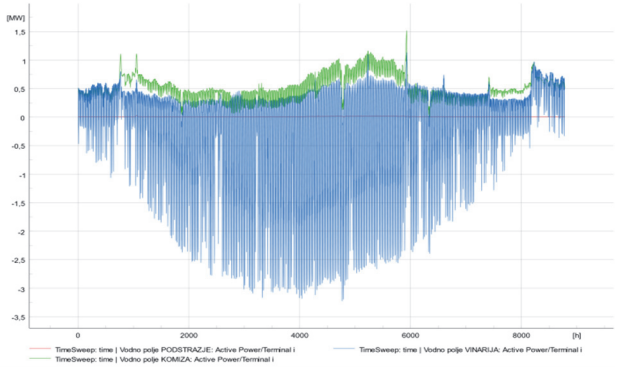

Figure 13 Island microgrid feeders power flows after PV+BESS integration

The integration of the PV power plant and BESS that is already in operation at the Vis island microgrid has resulted in a significant reduction in energy dependency on the upstream grid, with the PV power plant injecting 6062 MWh of energy. This integration has also resulted in improved voltage profiles and reduction losses.

4.3 Island Microgrid Simulation with an Integrated PV, BESS and Wavestar/Wavebob WECs at Both Locations

In this scenario WEC, island's grid with an integrated photovoltaic power plant and battery storage system, along with a WEC power plant at location 1 (Fig. 14 and Fig. 15), is designed to achieve near-zero power transfer with the upstream grid for two types of WECs. In order to achieve the 'net-zero'grid exchange 7 Wavestar WECs or 196 Wavebob WECs are needed in WEC power plant, connected at terminal "Podšpilje-Dračevo polje".

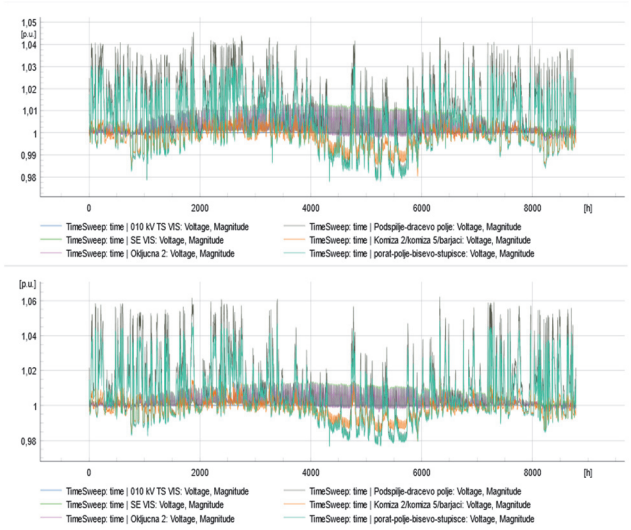

Figure 14 Island microgrid terminal buses voltage levels after PV + BESS + WECs integration at location 1 (up 7 Wawestars, down 196 Wavebobs)

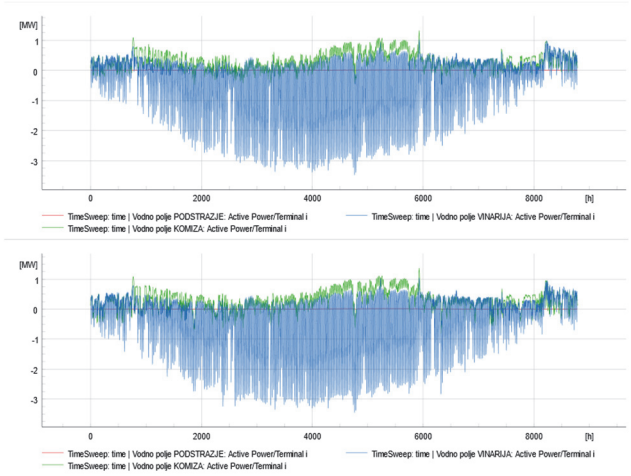

Figure15 Island microgrid feeders power flows after PV+BESS+WECs integration at location 1 (up 7 Wawestars, down 196 Wavebobs)

Integration of a WEC power plant has led to a nearly complete reduction in energy reliance on the upstream grid with the total imported energy of only 18 MWh for Wavestar power plant and less the 1 MWh for Wavebob power plant. The WEC power plant, consisting of Wavestar WECs, injected 3329 MWh of energy with a capacity factor of 36.09% and for Wavebob 3357 MWh of energy and a capacity factor of 24.96%. This integration has also resulted in improved voltage profiles and a reduction in grid losses on the island.

Similar simulations (Fig. 16 and Fig. 17) are performed for location 2, where 7 Wavestar WECs or 238 Wavebob WECs are now needed in WEC power plant connected to the grid at terminal "Oključna 2" in order to achieve the 'net-zero'grid exchange. On the location 2 the integration of a WEC has again led to near zero energy dependence on the upstream grid (326 MWh for Wavestar and 17 MWh for Wavebob, since WEC power plant injects 2845 MWh of energy with a capacity factor of 30.84% for Wavestar and 3223 MWh of energy with a capacity factor of 19.73% for Wavebob. There are some differences in power flow and voltage distribution due to the different locations but in general this integration has also resulted in improved voltage profiles and losses reduction as expected.

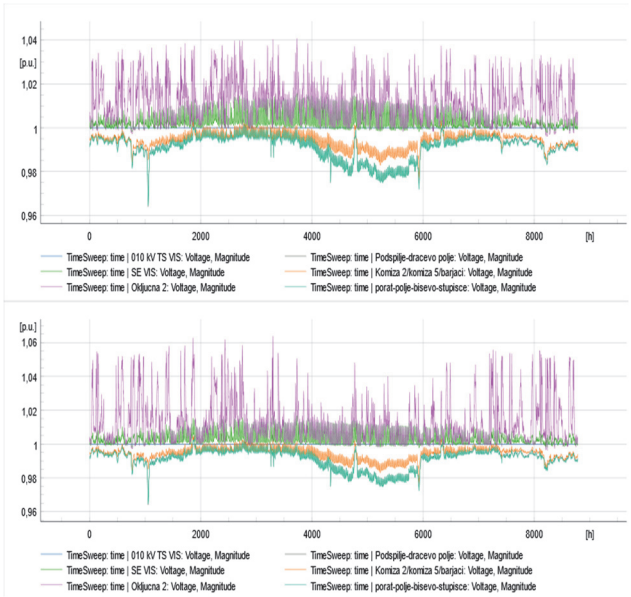

Figure 16 Island microgrid terminal buses voltage levels after PV + BESS + WECs integration at location 2 (up 7 Wawestars, down 238 Wavebobs)

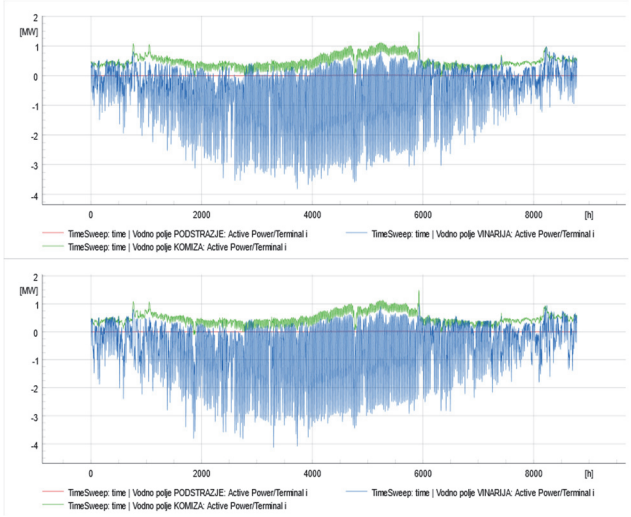

Figure 17 Island microgrid feeders power flows after PV + BESS + WECs integration at location 2 (up 7 Wawestars, down 238 Wavebobs)

4.4 Island Microgrid Simulation with an Integrated PV, BESS and Wavestar/Wavebob WECs with Adjacent BESS

For this scenario at location 1, a battery energy storage system (BESS) with a rated energy capacity of 5.5 MWh and 1 MW power rating has been installed alongside the wave converter power plant. BESS was modelled by the "battery storage" model in PowerFactory with appropriate time characteristic modelled by comparing the output power of WEC with an upper limit set value (0.8 MW for Wavestar and 1 MW for Wavebob). When the output power exceeded this limit, BESS is charged with the difference between the two values. If the output power of the WEC fell below the lower limit set value (0.4 MW for Wavestar and 0.5 MW for Wavebob) then BESS would be discharged by half the value of the difference between the lower limit value and the current output power of the WEC power plant. The intention was to employ BESS to mitigate the surges in production and to have a sustained positive power output from the combined WEC (WEC) and BESS during periods of diminished output. However, this would require a significantly bigger battery capacity and/or a more elaborate BESS control model.

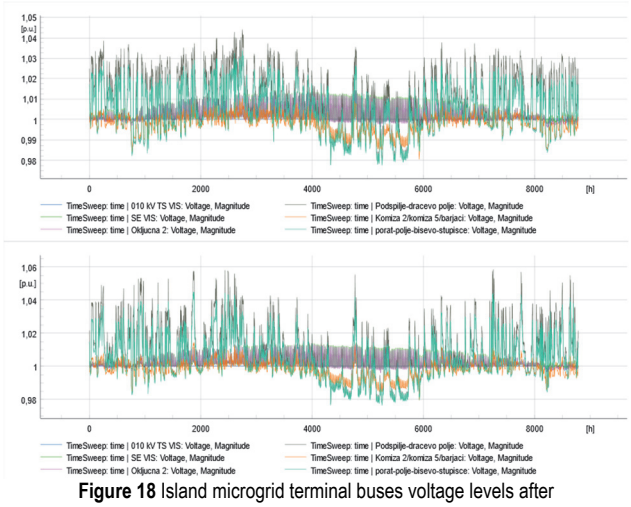

Figure 18 Island microgrid terminal buses voltage levels after PV + BESS + WECs with BESS integration at location 1 (up 7 Wawestars, down 196 Wavebobs)

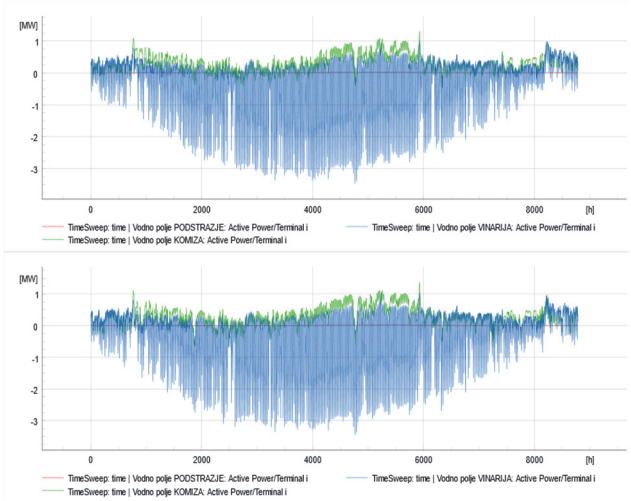

Figure 19 Island microgrid feeders power flows after PV + BESS + WECs with BESS integration at location 1 (up 7 Wawestars, down 196 Wavebobs)

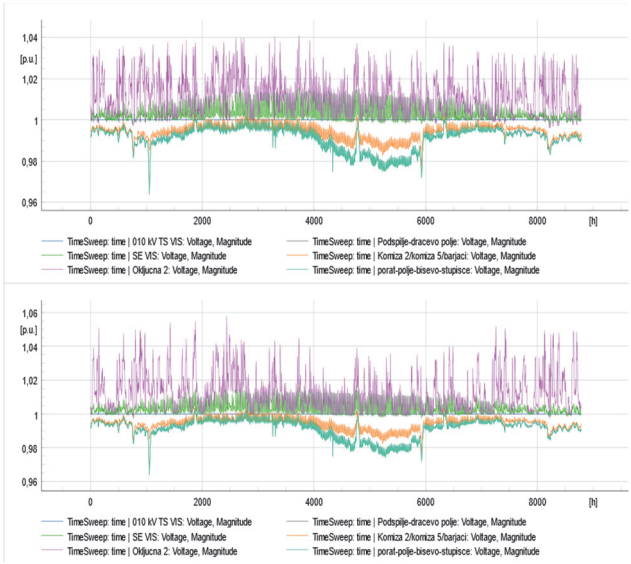

Figure 20 Island microgrid terminal buses voltage levels after PV + BESS + WECs with BESS integration at location 2 (up 7 Wawestars, down 238 Wavebobs)

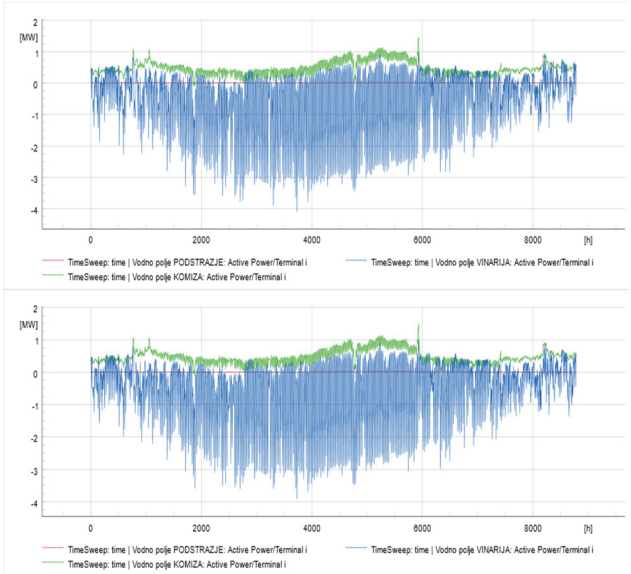

Figure 21 Island microgrid feeders power flows after PV + BESS + WECs with BESS integration at location 2 (up 7 Wawestars, down 238 Wavebobs)

Comparing results for both locations where the integrated battery system is now installed with the previous, it is obvious that the installation of additional adjacent BESS has resulted in a decrease in the maximum power output from the WEC power plant as intended. This reduction has led to reduction in the terminal buses voltage variations. At the same time, the power exchange with the upstream grid of the neighbouring island of Hvar has been, in general, reduced to achieve even closer to net-zero exchange.

5 CONCLUSION

Paper presented a successful possibility of integrating WECs to the microgrid of the island of Vis with the aim to archive near net zero electricity exchange with the mainland grid. Although the grid itself is fairly strong without any integrated distribution, simulation results indicate that in all scenarios the voltage quality has been

improved, especially on the electrically farthest terminal buses.

As for the power flows and over voltages on the distributed generation terminal buses where the PV and WECs were integrated, this can be further mitigated by implementing better BESS control where also the combination of RES with a BESS contributed to the reduction of the intermittency of the power flow, which has a positive effect on the grid and reduces dependency on the grid connection to the mainland. This kind of power-electronic-based device can be utilized in a different manner, such as a community-scale BESS connected at the beginning of the feeder to regulate active and reactive power flows with a reactive power provision to regulate loading and voltages.

Future research should focus on this, as well as on its influence on power quality indices, particularly flickers and harmonic distortion and cost-benefit analysis of the integration of WECs into island renewable microgrids.

Acknowledgements

This research (paper) has been supported by the Ministry of Science, Technological Development and Innovation through project no. 451-03-47/2023-01/200156 "Innovative scientific and artistic research from the FTS (activity) domain".

6 REFERENCES

[1] Pelc, R. & Fujita, R. M. (2002). Renewable energy from the ocean. *Marine Policy, 26*(6), 471-479 https://doi.org/10.1016/S0308-597X(02)00045-3

[2] Šljivac, D., Temiz, I., Nakomčić Smaragdakis, B., & Žnidarec, M. (2021).Integration of wave power farms into power systems of the Adriatic islands: technical possibilities and cross-cutting aspects. *Water, 13*(1), 13-28. https://doi.org/10.3390/w13010013

[3] Pecher, A. & Kofoed, J. P. (2017). *Handbook of Ocean Wave Energy*. Springer Open. https://doi.org/10.1007/978-3-319-39889-1

[4] Ning, D. & Ding, B. (2022). *Modelling and Optimization of Wave Energy Converters, First edition*. Boca Raton, London, New York: CRC Press. https://doi.org/10.1201/9781003198956

[5] Katalinić, M. (2019). *Modelling of Wind-Generated Waves in the Adriatic Sea for Applications in Naval Architecture and Maritime Transportation*. Doctoral Thesis, University of Zagreb, Zagreb.

[6] Madassery, N. J. (2017). Design and Layout of Power Conversion Chain for a Wave Energy Converter. *KTH Royal Institute of Technology,* Stockholm.

[7] Gobato, R., Gobato, A., & Fedrigo, D. F. G. (2015). *Study Pelamis system to capture energy of ocean wave*.

[8] 'Wave Dragon'. http://www.wavedragon.net (accessed Jun. 07, 2023).

[9] 'Archimedes Waveswing'.

[10] López, I., Andreu, J., Ceballos, S., Martínez de Alegría, I., & Kortabarria, I. (2013). Review of wave energy technologies and the necessary power-equipment. *Renewable and Sustainable Energy Reviews, 27*, 413-434. https://doi.org/10.1016/j.rser.2013.07.009

[11] López, I., Andreu, J., Ceballos, S., Martínez de Alegría, I., & Kortabarria, I. (2013). Review of wave energy technologies and the necessary power-equipment. *Renewable and Sustainable Energy Reviews, 27*, 413-434. https://doi.org/10.1016/j.rser.2013.07.009

[12] Pecher, A. & Kofoed, J. (2017). *Handbook of Ocean Wave Energy*. https://doi.org/10.1007/978-3-319-39889-1

[13] Jenkins, N., Kirschen, D., Strbac, G., Crossley, P., & Allan, R. (2000). Embedded Generation. *United Kingdom: IEE*.

[14] Bollen, M. H. J. & Hassan, F. (2011). Integration of Distributed Generation in the Power System. *Wiley-IEEE Press*. https://doi.org/10.1002/9781118029039

[15] Katalinić, M., Ćorak, M., Parunov, J. (2014). Analysis of wave heights and wind speeds in the Adriatic Sea. *London: Maritime Technology and Engineering-Guedes Soares & Santos (Eds)*. https://doi.org/10.1201/b17494-188

[16] Copernicus Climate Data Store. (2023) *New Climate Data Store (Beta) is live*. https://cds.climate.copernicus.eu/cdsapp#!/home

[17] 'GEBCO - The General Bathymetric Chart of the Oceans'. (2023). https://www.gebco.net

[18] Coe, R. G. & Neary, V. S. (2014). Review of Methods for Modeling Wave Energy Converter Survival in Extreme Sea States', Seattle. *Proceedings of the 2nd Marine Energy Technology Symposium*.

[19] Babarit, A., Hals, J., Muliawan, M. J., Kurniawan, A., Moan, T., & Krokstad, J. (2012). Numerical benchmarking study of a selection of wave energy converters, *Renew Energy, 41*, 44-63, https://doi.org/10.1016/j.renene.2011.10.002

[20] Prpić, L. (2021). Integracija postrojenja na morske valove na Jadranskim otocima u okviru WECANet projekta. *University of J. J. Strossmayer of Osijek,* Osijek.

[21] Žnidarec, M., Šljivac, D., Dosen, D., & Nakomcic-Smaragdakis, B. (2020). Performance evaluation of simple PV microgrid energy management system. *2020 International Conference on Smart Systems and Technologies (SST), Osijek, Croatia*, 213-218. https://doi.org/10.1109/SST49455.2020.9264129

[22] Javid, J., Li, K. J., Ul Hassan, R., & Chen, J. (2020).Hybrid-Microgrid Planning, Sizing and Optimization for an Industrial Demand in Pakistan. *Tehnički vjesnik, 27*(3), https://doi.org/10.17559/TV-20181219042529

Contact information:

Blaž JOZANOVIĆ
Josip Juraj Strossmayer University of Osijek,
Faculty of Electrical Engineering, Computer Science and Information Technology,
Kneza Trpimira 2b, 31000 Osijek, Croatia
E-mail: blaz.jozanovic@student.ferit.hr

Irina TEMIZ, Associate professor
Uppsala University,
Department of Electrical Engineering,
Box 65, 75103 Uppsala, Sweden
E-mail: Irina.temiz@uu.se

Damir ŠLJIVAC, Full Professor with tenure
Josip Juraj Strossmayer University of Osijek,
Faculty of Electrical Engineering, Computer Science and Information Technology,
Kneza Trpimira 2b, 31000 Osijek, Croatia
E-mail: damir.sljivac@ferit.hr

Branka NAKOMČIĆ SMARAGDAKIS, Full Professor
(Corresponding author)
University of Novi Sad, Faculty of Technical Sciences,
Trg Dositeja Obradovica 6, 21000 Novi Sad, Serbia
E-mail: nakomcic@uns.ac.rs